Characteristic Study of Shenmu Bituminous Coal Combustion with Online TG-MS-FTIR

Guanfu Pan[1, 2, 3]

[1] China Coal Research Institute Company of Energy Conservation Corporation Ltd..
[2] State Key Laboratory of Coal Mining and clean Utilization.
[3] National Energy Technology & Equipment Laboratory of Coal Utilization and Emission Control.
Address of all above: 5 Qingniangou east road, Hepingli Subdistrict, Beijing, China.
Email: panguanfubest@163.com

Abstract. The combustion characteristics of Shenmu bituminous pulverized coal (SBC) were comprehensively investigated with a combined TG-MS-FTIR system by considering the effect of particle size, heating rate and total flowrate. The combustion products were accurately quantified by normalization and numerical analysis of MS results. The results indicate that the decrease of the particle size, heating rate and total flowrate result in lower ignition and burnout temperatures. The activation energy tends to be lower with smaller particle size, lower heating rate and total flowrate. The MS and FTIR results demonstrate that lower concentrations of different products, such as NO, NO_2, HCN, CH_4 and SO_2 were produced with smaller particle size, slower heating rate and lower total flowrate. The decrease of particle size would lead to more contact area with oxygen and slower heating rate could provide more sufficient time for the diffusion. High total flowrate would reduce the oxygen adsorbability on the coal particle surface and shorten the residence time of oxygen, which makes the ignition difficult to occur. This work will guide to understand the combustion kinetics of pulverized coals and be beneficial to control the formation of pollutants.

1. Introduction

With the advantages of excellent thermal stability, high calorie and huge reserves, the Shenmu bituminous coal (SBC) has been adopted as one of the most widely used coal in China [1-3]. The investigation of the combustion characteristics is essential to understand the combustion process and control the pollutant products.

In recent years, SBC has been studied in terms of its burning and gasification properties. In 2003, Sun et al. [4] investigated the thermogravimetric (TG) characteristics of SBC and reported that vitrinite had higher volatile matter yield, maximum weight loss rate, lower initial decomposition temperature and peak temperature than that of inertinite. Compared to pressure and heating rate, the temperature has a more important impact on the devolatilization of SBC. With TG analysis, Zhao et al. [5] studied the ignition temperature (T_{ig}), maximum reaction temperature (T_{max}), burning rate, burnout temperature (T_{burn}) and combustion features of SBC coal and coke fine mixed sample. The results showed that with the increasing of the coke fine content, T_{ig} of the coal and coke fine mixture, the caloric value of the sample and the T_{max} would increase, while the burning rate would decrease. Yang et al. [6] studied the SBC ash's physicochemistry with temperature on the basis of TG-differential scanning colorimetry (TG-DSC) methods. The results indicated that the SBC ash could convert into a eutectic at low temperatures. Chang et al. [2] investigated the formation of nitrogeneous products from the gasification of SBC in a fluidized-bed/fixed-bed reactor. More recently, Yang et al. [7]

investigated the SBC's characteristics of combustion and nitrogen oxide (NOx) release in a fixed-bed reactor. The composition of the flue gas was analyzed to investigate the effect of sodium acetate on the combustion process and NOx emission. Sodium acetate was observed to reduce NOx emissions due to their special reactions with the nitrogen-containing species.

Although some works related to the combustion studies of SBC are available, a systematic study regarding the effect of particle size, heating rate and total flowrate on its combustion characteristics is scarce. Mass spectrometry (MS) and Fourier transform infrared spectroscopy (FTIR) are widely used in multicomponent analysis in energy chemical industry and are suitable to be combined with TG and gas chromatographic method [8]. It is efficient and reliable to use the TG-MS-FTIR system for numerical analysis of the combustion characteristics of coal. In the current work, the combustion characteristic of SBC was comprehensively studied with online TG-FTIR-MS system. The products formed in the combustion of SBC were accurately qualified and quantified by considering the electron impact ionization cross sections, ion flow intensities and the partial pressures of different species. The condition-characteristic relationship among the particle size, heating rate and total flowrate and ignition, burnout temperature as well as activation energy was addressed.

2. Materials and Methods

2.1. Coal Samples

The SBC samples were bought from Shenmu Energy Developments Ltd Company and grinded into powder with different sizes. Before test, the sample was put into drying oven at the temperature of 105 °C for 90 min. Then the coals were sieved to a particle size of lesser than 40, 90-100, 128-180, 280-355 and 355-500 μm. The coal samples are mainly composed of $CaCO_3$, SiO_2 and Kaolinite, as shown in Figure. 1. The existence of carbonate could be the main reason to form the weak weight loss peak at the end of the combustion processes.

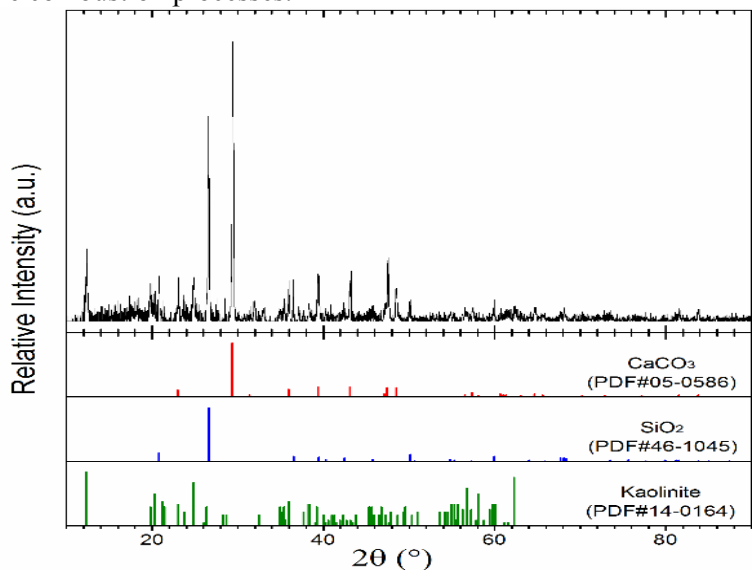

Figure 1. XRD patterns of SBC.

The elements of SBC samples were identified by the coal proximate analyzer as shown in Table I.

Table 1. The proximate analysis and ultimate analysis results of SBC.

Proximate analysis					**Ultimate analysis**				
M_{ad}	A_{ad}	V_{ad}	FC_{ad}	$Q_{ad.net}$	C_{ad}	H_{ad}	O_{ad}	N_{ad}	S_{ad}
%	%	%	%	kJ/kg	%	%	%	%	%
6.53	10.41	32.40	50.66	26120	66.70	4.11	10.79	1.04	0.42

2.2. Comprehensive Test

The tests of SBC combustion characteristics were performed with the TG-MS-FTIR system which comprises a TG analyzer (STA-449F3, Netzsch), a mass spectrometer (QMS403C, Aeolos) and an FTIR spectrometer (Tensor 27, Bruker). The combined system was controlled simultaneously and data were recorded by a computer, as shown in Figure. 2.

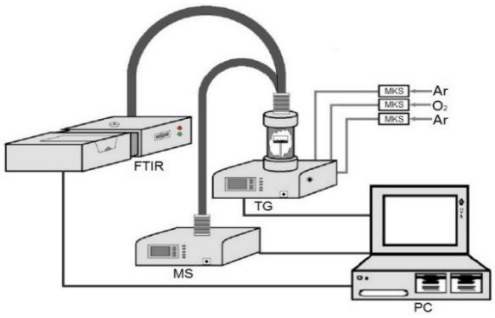

Figure 2. Scheme of TG-MS-FTIR system.

The tests were carried out in four steps. Firstly, about 10 mg sample was dispersed on a circular alumina pan and the air in TG chamber was replaced with a gas contained 20 % O_2 and 80 % Ar. So O_2 was more than the theoretically needed for the SBC combustion. Secondly, the samples were heated with a heating rate of 10 °C/min from 40 to 110 °C and kept for 30 min. Thirdly, the samples were heated to 1200 °C by four heating rate, namely 10, 20, 30 and 40 °C/min, respectively. Finally, the whole temperature-rising program was finished after an isothermal process of 10 min. Three total flowrates (50, 100 and 150 sccm) containing 20 % O_2 and 80 % Ar were sent into the TG chamber during the whole heating processes. The detailed experimental conditions are summarized in Table 2.

Table 2. Experimental conditions

Condition	Mass (mg)	Flowrate (sccm)			Heating rate (°C/min)	Particle size (μm)
		O_2	Ar	Ar		
1	9.411	20	60	20	20	0-40
2	10.248	20	60	20	10	90-100
3	9.788	20	60	20	20	90-100
4	9.348	20	60	20	30	90-100
5	9.589	20	60	20	40	90-100
6	9.251	20	60	20	20	125-180
7	10.246	20	60	20	20	280-355
8	9.786	20	60	20	20	355-500
9	9.341	10	20	20	20	90-100
10	9.864	30	100	20	20	90-100

2.3. Data Treatment

2.3.1. *Characteristic Temperature.* The ignition characteristic of SBC is analyzed based on T_{ig}. In the present work, T_{ig} is determined by the commonly recognized TG-DTG methods [9]. The T_{burn} is defined as the temperature with 98% total weight loss. The T_{max}, referring to the temperature at which combustion product own maximum volumetric flow, was also determined through numerical analysis.

2.3.2. *Kinetic Analysis.* The combustion kinetic parameters from TG data is calculated by the Coats-Redfern method [10]:

n=1
$$\ln\left[\frac{-\ln(1-\alpha)}{T^2}\right] = \ln\left[\frac{AR}{\beta E}\left(1-\frac{2RT}{E}\right)\right] - \frac{E}{RT} \quad (1)$$

n≠1
$$\ln\left[\frac{1-\ln(1-\alpha)^{1-n}}{T^2(1-n)}\right] = \ln\left[\frac{AR}{\beta E}\left(1-\frac{2RT}{E}\right)\right] - \frac{E}{RT} \quad (2)$$

where $\alpha = (m_0 - m)/(m_0 - m_\infty)$ is the weight loss ratio; m refers to the sample mass; m_0 and m_∞ represent the initial mass and the final mass, respectively; β is heating rate, K·min^{-1}; R is the gas constant; E stands for activation energy, $J{\cdot}mol^{-1}$; A is the frequency factor, min^{-1}; n refers to the order of reaction. In general, the item $\frac{2RT}{E} << 1$ and $(1-\frac{2RT}{E}) \approx 1$. As the first item of the right side of equations is nearly a constant, the two equations should result in a straight line of slope. E can be deduced through calculation with the slope.

2.3.3. Products Analysis. To obtain the volumetric flowrates of the products during the oxidation of SBC, both MS and FIIR were used. In order to give accurate quantitative analysis, a novel method of equivalent characteristic spectrum analysis was employed and the details of such method can be found elsewhere [11]. In the MS analysis, argon was used as a reference gas to calibrate the products by considering the electron impact ionization cross sections, ion flow intensities and the partial pressures of different species. The characteristic spectra and relative sensitivity were deduced. The effect of initial coal weight on the formation of products was excluded by normalization of the coal weight. The relative uncertainty of calculated MS results was estimated to be 0.052 [11].

3. Results and Discussion

3.1. TG/DTG Results

Figure 3 presents the TG/DTG curves obtained in the combustion of SBC samples. As temperature increases, the coal sample could proceed with several steps, including devolatilization, coke formation and coke combustion. The peak of maximum weight loss moves towards high temperatures gradually and the peak value decreases slightly as the particle size increases. The combustion rate depends on the diffusion and reaction ability. During the rapid combustion processes, the major factor affecting the combustion is diffusion ability. As the particle size increases, the contact surface area decreases, which would inhibit the diffusion of oxygen and make the devolatilization and combustion difficult. So the devolatilization occurs at higher temperature and the value of weight loss peak decreases.

Compared to particle size, heating rate has more apparent effect on the characteristics of weight loss. As the heating rate increases, the peak of weight loss moves towards high temperatures. In addition, the peak values and residues decrease as well. Since diffusion ability is the dominant factor in affecting the combustion process, longer contact time of sample surface and oxygen could contribute to SBC conversion. Thus, the burnout time with low heating rate is longer. Sufficient contact of particles and oxygen is beneficial for the combustion process, and the maximum value of weight loss occurred at lower temperatures and the maximum weight loss shifted to larger values [12]. It is clearly that there is a small weight loss peak within 600~700 °C. This weak peak could come from the decomposition of carbonate in the coal samples. In addition, the TG/DTG results of different total flowrates are observed to be quite similar, as displayed in Figure. 4e and f. As the oxygen supplied is much more than the theoretical needed for the complete combustion, the weight loss characteristics are insensitive to the diverse total flowrate changed in experiments.

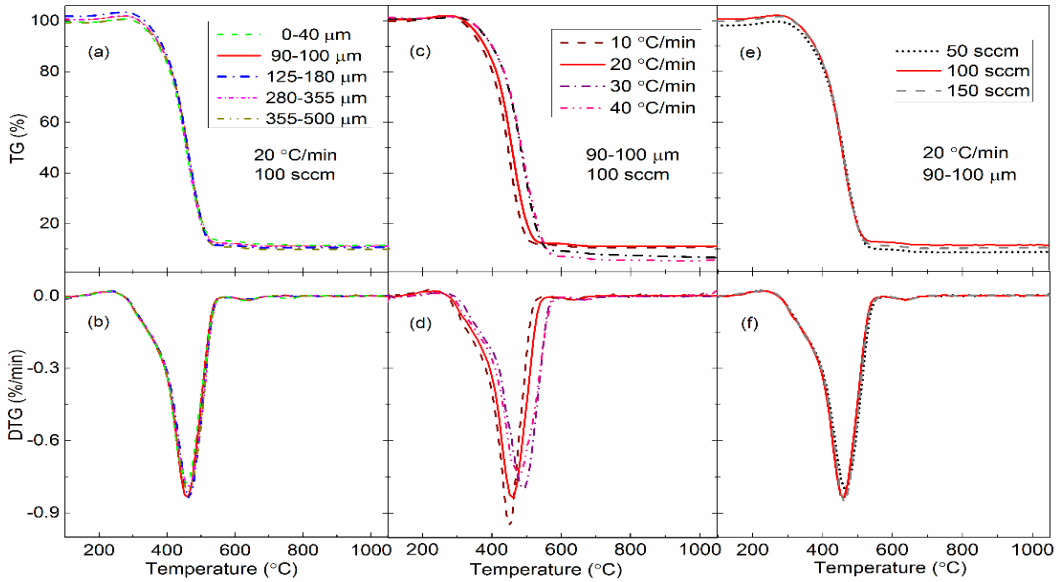

Figure 3. TG and DTG curve of SBC combustion with different particle size, heating rate and total flowrate.

3.2. Characteristic Temperatures

The characteristic temperatures obtained in the combustion of SBC at different particle sizes, heating rates and total flowrates are shown in Figure. 4. As indicated in Figure. 4a, both T_{ig} and T_{burn} fall down as the particle size decreases, which is consistent with the results reported by Zhang et al. [13] for Yuanbaoshan and Datong coal and Zhou et al [14] for Lengshuijiang coal and lean coal. According to Zhang et al. and Zhou et al., the decrease of particle size could lead to larger surface area to expose to oxygen. The same behavior could occur to SBC and the larger surface area of SBC sample with smaller particle size would endow it with lower T_{ig} and T_{burn}.

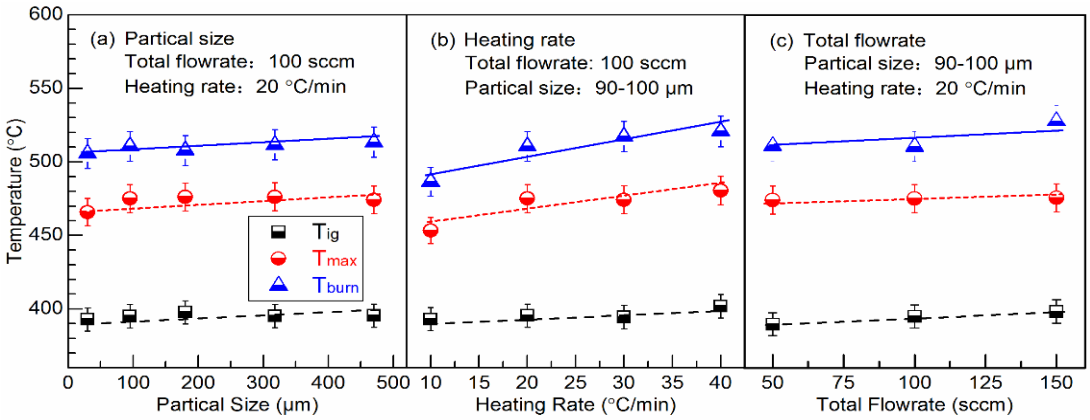

Figure 4. Characteristic temperatures of SBC combustion with different particle size, heating rate and total flowrate.

Figure 4b displays the characteristic temperature as a function of heating rate. The T_{ig}, T_{max} and T_{burn} tend to decrease slightly as the heating rate decreases, which agrees well with the conclusion drawn by Lu et al. [15] for Qilianta coal. This is due to the fact that the thermal conduction in coal particle at lower heating rate is better than that at higher ones. With the temperature increasing, the diffusion becomes better, which is helpful to the devolatilization and results in lower T_{ig}. Moreover, the reaction time is more sufficient at slower heating rate. As the plugging of the surface pores is avoided, it is more difficult to form ash cladding, which could give rise to a lower T_{burn} [16].

For the total flowrate, a slight increase of T_{ig} is observed with large total flowrate (see Figure. 4c). This slight increase mainly comes from shorter residence time of O_2 on the surface of coal particles at higher total flowrate. Even though more oxygen reached the coal surface, the higher speed of oxygen molecule makes the adsorption of oxygen more difficult. As the supplied O_2 was much more than the theoretically needed for the complete oxidation of the SBC sample, the influence of oxygen flow on the complete combustion and maximum combustion speed is not obvious. As a consequence, both T_{max} and T_{burn} exhibit similar values in the combustion of SBC at different total flowrates.

3.3. Activation Energy

Figure 5 summarizes *E* of SBC with variation of particle size, heating rate and total flowrate. *E* tends to be low with the decrease of particle size, heating rate and total flowrate. As the particle size decreases, the surface area increases, which would result in more contact area with oxygen and better thermal reactivity. Thus, energy transfer from outside into inner becomes more rapidly, and *E* is getting low. Lower heating rate will make the energy transfer more evenly and slow down the rate of surface ash generating. When the total flowrate rises, the contact time of oxygen and sample surface will be shortened and result in increase of E. The lower energy barrier makes the oxidation occur more easily [17-19]. This finding also shows good agreement with the conclusion drawn by Lu et al. [15] for different kinds of coal. Similar to the tendency of T_{ig}, E decreased when the total flowrate turned lower. The adsorbability of oxygen on the coal particle surface is better with lower total flowrate, which could be responsible for the decrease of energy barrier.

3.4. MS and FTIR Results

The volumetric flows of combustion products at different temperatures can be obtained by normalization and numerical analysis of MS results. The maximum volumetric flows of different combustion products as well as the corresponded temperatures (T_{max}) are used to explore the formation rule of emitted pollutants. Table 3 shows the maximum volumetric flows of CH_4, NH_3, NO, HCN, NO_2 and SO_2 as well as the corresponded temperatures (T_m). By comparing the results obtained with different particle size, the listed species tend to be less produced with smaller particle size. In view of the heating rate, lower amounts of these products were measured at lower heating rate. As far as the total flowrate is concerned, the quantity of these species becomes lower when the total flowrate is smaller. In general, the T_m is insensitive to the particle size. However, the increase of the total flowrate normally results in smaller Tm. With the increase of the heating rate, T_m of NO, NH_3 and HCN tends to be higher, while Tm of SOx is getting lower. To summarize, lower concentrations of CH_4, NH_3, NO, HCN, NOx and SO_2 were observed at smaller particle size, slower heating rate and bigger total flowrate.

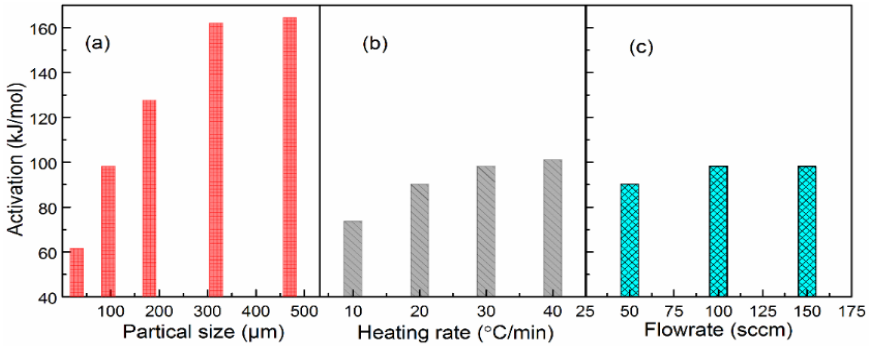

Figure 5. Activation energies of SBC combustion with different particle size, heating rate and total flowrate.

Figure 6 shows the volumetric flowrates of species formed under condition 4 (see Table 2). In the combustion of SBC, both NH_3 and HCN exhibited two-peak shapes. The peak before T_{ig} comes from

the devolatilization, whereas the peak after T_{ig} results from the decomposition of nitrogen components in volatile and char. Further increase of the temperature led the conversion of NO and NO_2.

NO_2 exhibited a shoulder peak and an asymmetric single peak. The shoulder peak is due to the weak release of NO_2 during devolatilization. The asymmetric single peak could come from the conversion of nitrogen-containing heterocyclic species at the end of devolatilization and the beginning of char combustion. However, the other nitrogenous components enriched in char will release NO_2 during the rapid combustion of char. Less NO_2 emissions were observed at smaller particle size, slower heating rate and higher total flowrate. Similarly, the emissions of SO_2 are relatively less than those formed with slower heating rate and higher total flowrate. However, the amount of SO_2 is quite similar for the investigated particle size range, indicating that it is insensitive to the particle size.

Table 3. Maximum volumetric flow of representative combustion products

No.	CH_4		NH_3		NO		HCN		NO_2		SO_2	
	Value (slm)	T_m (°C)	Value (slm)	T_m (°C)	Value (slm)	T_m (°C)	Value (slm)	T_m (°C)	Value (slm)	T_m (°C)	Value (slm)	T_m (°C)
1	4.08E-05	442	3.61E-04	318	4.72E-05	493	5.05E-04	452	6.14E-05	431	6.38E-06	400
2	3.53E-05	427	2.41E-04	309	3.56E-05	458	3.68E-04	443	4.17E-05	438	4.52E-06	402
3	5.91E-05	440	2.81E-04	305	7.69E-05	492	3.09E-04	451	6.41E-05	440	7.73E-06	388
4	6.51E-05	437	2.17E-04	307	6.46E-05	494	4.94E-04	453	9.84E-05	429	8.37E-06	379
5	5.06E-05	430	3.41E-04	337	1.40E-04	507	3.97E-04	512	1.29E-04	439	1.24E-05	350
6	7.27E-05	453	4.23E-04	338	4.60E-05	494	6.74E-04	463	7.10E-05	442	4.55E-06	400
7	7.94E-05	453	4.89E-04	306	6.97E-05	504	5.19E-04	453	7.43E-05	442	6.33E-06	410
8	7.96E-05	432	3.73E-04	317	4.95E-05	503	4.52E-04	463	7.20E-05	442	6.20E-06	390
9	9.75E-05	453	7.72E-04	327	9.44E-05	504	6.53E-04	463	1.47E-04	453	1.01E-05	400
10	3.76E-05	430	1.58E-04	316	4.32E-05	482	3.03E-04	472	4.99E-05	440	5.75E-06	398

Note: T_m refers to the temperature at which the peak flow is obtained.

By comparing the formation of NO_2 and SO_2 with different particle sizes, heating rates and total flowrate shown in Figure. 7, it is obvious that the amount of SO_2 production is much lower than those of NO and NO_2. To summarize, the SBC combustion with smaller particle size, slower heating rateand bigger total flowrate is beneficial to controlling the formation of pollutants. This finding is consistent with the results reported for Hegang, Tiefa and Zhungeer coal [20] and Heshan sulfer coal. [18, 21].

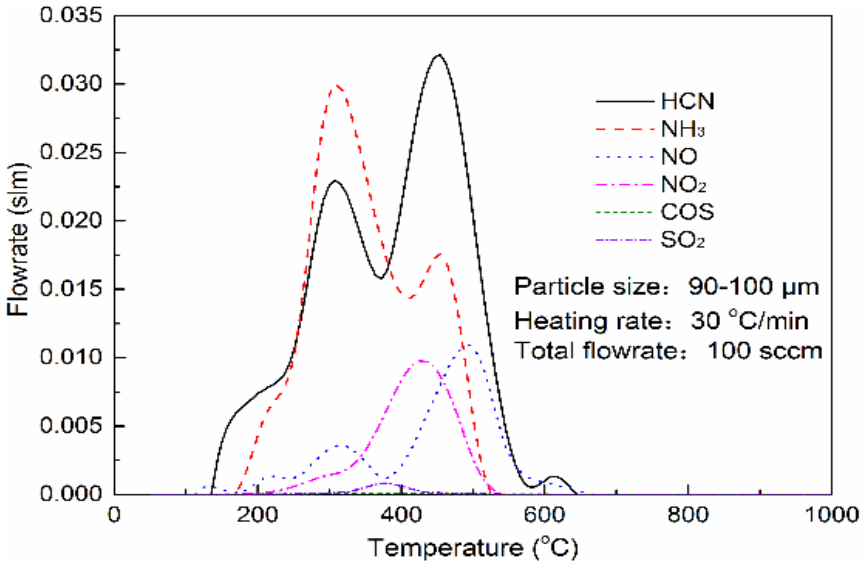

Figure 6. Flowrates of major products.

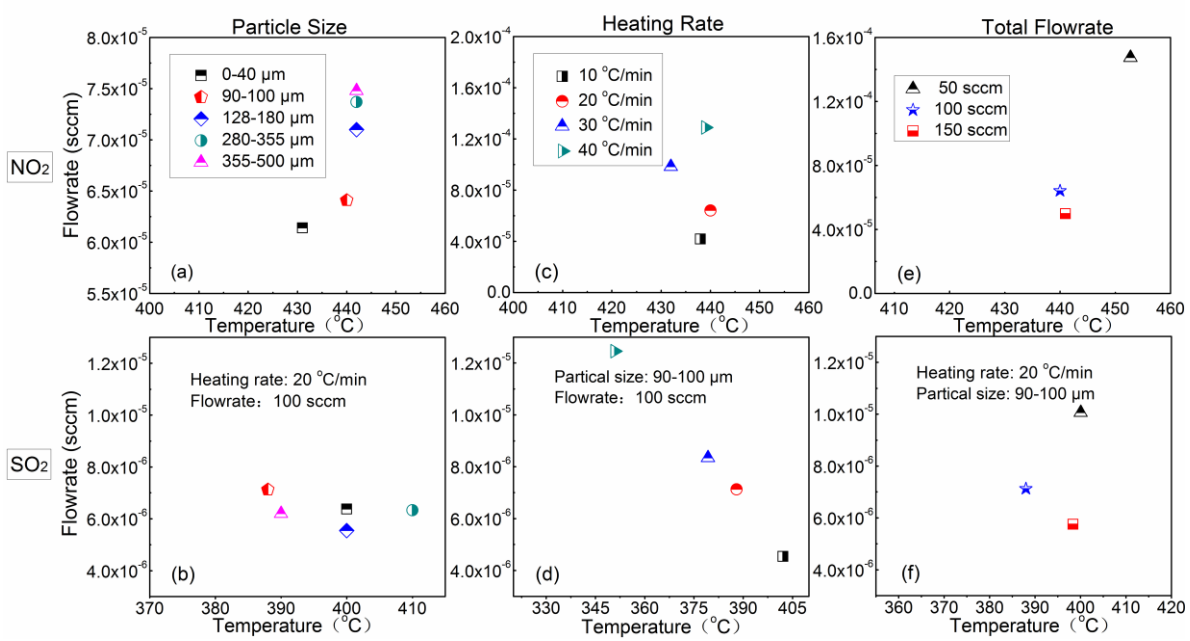

Figure 7. Production of NO_2 (a, c, e) and SO_2 (b, d, f) with different particle size, heating rate and total flowrate.

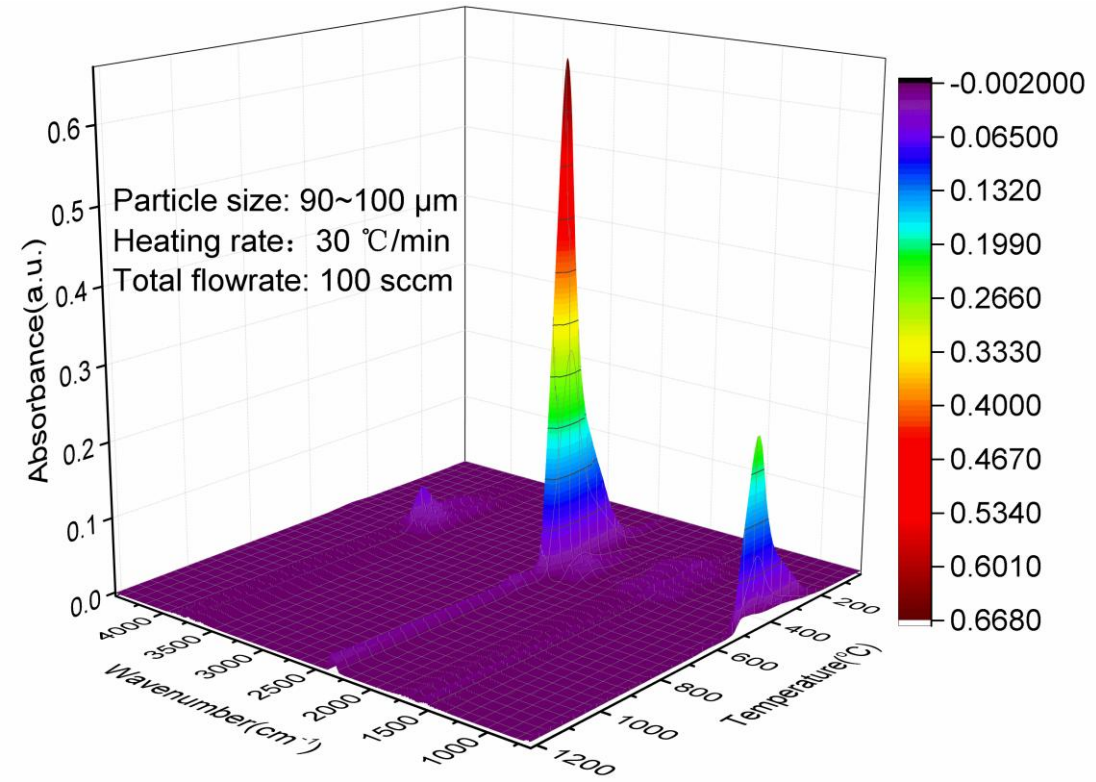

Figure 8. FTIR spectra with different wavenumber and temperature.

To visualize the formation of the major species and avoid the effect of ion fragmentation in MS, FTIR with spectral range of 500-5000 cm^{-1} was involved. Figure 8 presents a representative three-dimensional spectrum measured with particle size of 90-100 μm and heating rate of 30 °C/min. The maximum absorbance peak is located at the wavenumber of 2380 cm^{-1} corresponding to the

anomalistic vibration of CO_2. Another obvious peak at 700 cm^{-1} belongs to the bending vibration of CO_2. The peaks at 1375 and 3600 cm^{-1} corresponds to SO_2 and H_2O, respectively. By comparing the standard spectral peaks of different species, overlapped peaks were observed. For instance, the peak between 1500-1800 cm^{-1} was the overlap of H_2O and NO [22, 23]. In Figure. 8, CO_2 becomes detectable at around 140 °C. Up to 200 °C, a slow increase was observed. Another turning point was measured at about 375 °C, which also agrees well with the wave valley in the profiles of HCN and NH3. Besides CO_2, the fast production of the major species was achieved within the temperature range of 400-500 °C, which is consistent with the rapid combustion temperature revealed in the MS analysis.

4. Conclusion

The combustion of SBC was comprehensively studied with online TG-FTIR-MS system in terms of characteristic temperatures as well as qualitative and quantitative analysis of products. Five particle sizes ranging from 0-500 μm, four heating rates from 10 to 40 °C/min and three total flowrate from 50-150 sccm were used. To avoid the influence of overlap peaks, signal drift and dynamic response delay in ion current spectra during MS analysis, argon was used as a reference gas to calibrate the products by considering the electron impact ionization cross sections, ion flow intensities and the partial pressures of different species. The results indicate that the decrease of the particle size, heating rate and flowrate lead to lower ignition and burnout temperatures, and the activation energy tends to be lower with smaller particle size, slower heating rate and lower flowrate. The decrease of particle size could lead to more contact area with oxygen and better thermal reactivity. Slower heating rate could provide more sufficent time for the reaction. Moreover, higher total flowrate would reduce the oxygen adsorbability on the coal particle surface at higher flow speed. From MS and FTIR analysis, lower concentrations of different products were observed to be formed at smaller particle size, slower heating rate and higher total flowrate. These findings will guide to understand the combustion kinetics of SBC and be beneficial to control the formation of pollutants.

5. Acknowledgments

The author thanks the financial support from youth fund of China Coal Technology & Engineering Group Corp (No. 2018QN004).

6. References

[1] J Cheng, JH Zhou, JZ Liu, XY Cao, KF Cen. 2009 *Energy Sources Part a-Recovery Utilizatio and Environmental Effects*. 31p 956-66.
[2] LP Chang, KC Xie, CZ Li. 2004 *Fuel Processing Technology*. 85 p 1053-63.
[3] XM Wang, YQ Jiao, LQ Wu, H Rong, *XM Wang, J Song. Ordos Basin.* 2014 Fuel. 136p 233-9.
[4] Ql Sun, W Li, HK Chen, BQ Li. 2003 *Journal of China University of Mining & Technology*. 32p 664-9.
[5] SY Zhao. 2007 *Coal Science and Technology*. 35 p 80-2.
[6] JG Yang, FR Deng, H Zhao, KF Cen. 2007 *Asia-Pacific Journal of Chemical Engineering*. 2 p 165-70.
[7] WJ Yang, JH Zhou, MS Liu, ZJ Zhou, JZ Liu, KF Cen. 2007 *Energy & Fuels.* 21p 2548-54.
[8] T Dijkmans, MR Djokic, KMV Geem, GB Marin. 2015 *Fuel*. 140p 398-406.
[9] QM Yu, YJ Pang, HG Chen. 2001 *North China Electric Power*. p 9-10+50.
[10] JP Redfern, AW Coats. 1964 *Nature Biotechnology*. 201p 68-9.
[11] HD Xia, K Wei. 2014 Thermchimica Acta, 602 15-21.
[12] SQ Wang, YG Tang, HH Schobert, GD Mitchell, FR Liao, ZZ Liu. 2010 *International Journal of Coal Geology*. 81p 37-44.
[13] CQ Zhang, LJ Yu, ZG Cui, XM Jiang. 2005 *Journal of Chemical Industry and Engineering*. 56 p 2189-94.
[14] Z hou, L Liu, YL Wang, H Liu. 2007 *Thermal Power Generation*. 3 p 35-8+47.
[15] HB Lu, HJ Xu, CX Jia, DL Zhang. 2006 *Power System Engineering*. 22 p 11-2+5.
[16] MS Nyathi, M Mastalerz, R Kruse. 2013 *International Journal of Coal Geology*. 118 p 8-14.

[17] DM Fan, ZP Zhu, YJ Na, QG Lu. 2012 *Journal of Thermal Analysis and Calorimetry*. 113p 599-607.
[18] XM Jiang, JB Li, JR Qiu. 1999 *Journal of China Coal Society*. 24 p 643-7.
[19] S Lu, GJ Lu, XG Jiang, Y Chi, JH Yan, KF Cen. 2014 *Journal of Coal Science & Engineering*. 3 p 554-61.
[20] LH Wei, XM Jiang, TH Yang, YJ Li, L Wang. 2006 *Acta Scientiae Circumstantiae*. 11 p 1780-4.
[21] XM Jiang, H Liu, JB Li, CG Zheng, DC Liu. 2002 *Environmental Science & Technology*. 23 p 126-8.
[22] T Ahamad, SM Alshehri. 2012 *Journal of Hazardous Materials*. 199 p 200-8.
[23] S Silvera. 2013 *Journal of Analytical and Applied Pyrolysis*. 104 p 95-102.